Computers and Geosciences 128 (2019) 19–29

Contents lists available at ScienceDirect

Computers and Geosciences

journal homepage: www.elsevier.com/locate/cageo

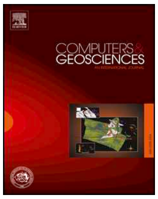

IGUG: A MATLAB package for 3D inversion of gravity data using graph theory

Saeed Vatankhah[a,*,1], Vahid Ebrahimzadeh Ardestani[a,2], Susan Soodmand Niri[a,3], Rosemary Anne Renaut[b,4], Hojjat Kabirzadeh[c,5]

[a] Institute of Geophysics, University of Tehran, Tehran, Iran
[b] School of Mathematical and Statistical Science, Arizona State University, Tempe, AZ, USA
[c] Department of Geomatics Engineering, University of Calgary, AB, Canada

ARTICLE INFO

Keywords:
Gravity
3D inversion
Graph theory
Equidistance function
Mobrun

ABSTRACT

We present an open source MATLAB package, IGUG, for 3D inversion of gravity data. The algorithm implemented in this package is based on methodology that was introduced by Bijani et al. (2015). A homogeneous subsurface body is modeled by an ensemble of simple point masses. The model parameters are the Cartesian coordinates of the point masses and their total mass. The set of point masses, assumed to each have the same mass, is associated to the vertices of a weighted complete graph in which the weights are computed by the Euclidean pairwise distances separating vertices. Kruskal's algorithm is used to solve the minimum spanning tree (MST) problem for the graph, yielding the reconstruction of the skeleton of the body described by the model parameters. The algorithm is stabilized using an equidistance function that restricts the spatial distribution of point masses and favors a homogeneous distribution for the subsurface structure. The non-linear global objective function for the model parameters comprises the data misfit term and the equidistance stabilization function. A regularization parameter λ is introduced to balance the two terms of the objective function, and reasonable physically-relevant bound constraints are imposed on the model parameters. A genetic algorithm is used to minimize the bound constrained objective function for a fixed λ, subject to the bound constraints. A new diagnostic approach is presented for determining a suitable choice for λ, requiring a limited number of solutions for a small set of λ. This contrasts the use of the L-curve which was suggested for estimating a suitable λ in Bijani et al. (2015). Simulations for synthetic examples demonstrate the efficiency and effectiveness of the implementation of the algorithm. It is verified that the constraints on the model parameters are not restrictive, even with less realistic bounds acceptable approximations of the body are still obtained. Included in the package is the script GMD.m which is used for generating synthetic data and for putting measurement data in the format required for the inversion implemented within IGUG.m. The script Diagnostic_Results.m is included within IGUG.m for analyzing and visualizing the results, but can also be used as a standalone script given import of prior results. The software can be used to verify the simulations and the analysis of real data that is presented here. The real data set uses gravity data from the Mobrun ore body, north east of Noranda, Quebec, Canada.

1. Introduction

The inversion of gravity data is an efficient methodology for estimating an approximate model of a subsurface body. Acquired gravity data on, or near, the surface are used in an automatic algorithm to estimate the defining model parameters, such as the density contrast

[*] Corresponding author.

E-mail addresses: svatan@ut.ac.ir (S. Vatankhah), ebrahimz@ut.ac.ir (V.E. Ardestani), susan.soodmand@ut.ac.ir (S.S. Niri), renaut@asu.edu (R.A. Renaut), hkabirza@ucalgary.ca (H. Kabirzadeh).

[1] Contribution: Dr. Vatankhah provided the flowchart for inversion steps and some associated codes.

[2] Contribution: Prof. Ardestani devised the project, the main conceptual ideas, and analysed the real data results.

[3] Contribution: Susan Soodmand worked on genetic algorithm parameters and associated codes, and carried out the synthetic and real case tests.

[4] Contribution: Prof. Renaut developed the regression analysis for determining the regularization parameter, the associated codes and is maintaining the software page.

[5] Contribution: Dr. Kabirzadeh analysed both synthetic and real data, with some suggestions on developed codes.

https://doi.org/10.1016/j.cageo.2019.03.008
Received 30 September 2018; Received in revised form 21 February 2019; Accepted 27 March 2019
Available online 01 April 2019
0098-3004/ © 2019 Elsevier Ltd. All rights reserved.

and geometry of the subsurface body. Using well-defined prior information in the inversion algorithm, an acceptable reconstruction for the subsurface is desired. Inversion methodologies include both linear and non-linear approaches, dependent on how the model is formulated. A standard linear inversion assumes that the subsurface under the survey area is discretized as a large number of prisms of known and fixed geometry. Then, the unknown density contrasts of each prism are estimated and displayed to illustrate the complete geometry and density of the subsurface sources (Last and Kubik, 1983; Li and Oldenburg, 1998; Portniaguine and Zhdanov, 1999; Boulanger and Chouteau, 2001; Vatankhah et al., 2017). This methodology provides sufficiently useful estimates of the subsurface for high confidence mineral exploration studies (Liu et al., 2015). On the other hand, non-linear gravity inversion is usually used to find interfaces. For example, in hydrocarbon exploration it is important to accurately identify the depth to the basement. Then, the geometry of the sedimentary basin is replaced with a series of juxtaposed prisms, of fixed width and known density contrast, but with unknown thickness. The shape of the sedimentary basin is obtained by estimating the thickness of each prism (Bott, 1960; Blakely, 1995; Chakravarthi and Sundararajan, 2007). Aside from these two standard approaches, other specialized techniques have been designed to handle particular situations. For example, Bijani et al. (2015) developed a graph theory approach for the 3D inversion of gravity data in which the subsurface body is modeled as an ensemble of simple point masses, of equal mass. The model parameters are the Cartesian coordinates and total mass of the point masses, and the algorithm yields the reconstruction of the skeleton of the body with the obtained coordinates and total mass. Here, as described in the following sections, we present a MATLAB package to implement gravity inversion based on extensions of the graph theory approach of Bijani et al. (2015).

It is well-known using the theory of Green's equivalent layer, that the solution of the gravity inverse problem is non-unique (LaFehr and Nabighian, 2012). Moreover, the gravity data measurements are always contaminated by noise due to both instrumental errors and modeling simplifications. Thus, in obtaining a geologically plausible solution given the measured data, prior information has to be incorporated into the solution process. A stabilizing regularization term is imposed to assure that the solution is not overly contaminated by noise in the data. This biases the search space for the model parameters to a space defined by the interpreter. For example, as used in linear inversion, L_0 and L_1 norm stabilizers lead to the reconstruction of sparse solutions (Last and Kubik, 1983; Portniaguine and Zhdanov, 1999; Boulanger and Chouteau, 2001; Vatankhah et al., 2015, 2017), a depth weighting function reduces the impact of the natural decay of the sensitivity matrix with depth (Li and Oldenburg, 1998), and imposed L_2 norm stabilization with a derivative operator provides smooth solutions (Li and Oldenburg, 1998). Non-linear inversions have been stabilized by constraining the density variation with depth (Chakravarthi and Sundararajan, 2007) and applying a total variation regularization (Martins et al., 2011). In the graph theory approach of Bijani et al. (2015) the equidistance function stabilization was introduced. The set of point masses are associated to the vertices of a weighted complete graph in which the weights between pairwise vertices are computed from the Euclidean distances between the vertex pairs. Kruskal's algorithm is used to solve the minimum spanning tree (MST) problem for the graph, and the equidistance function is computed using the MST. This function restricts the spatial distribution of the point masses and thus provides a solution that prefers a homogeneous spatial distribution for a single subsurface structure. Consequently, a skeleton of the body is reconstructed. We note that it is also possible to impose physically realistic bound constraints on the model parameters, determined by knowledge of the local geology.

General gravity inversion incorporating stabilization requires the minimization of an objective function comprising the data misfit term and the stabilizing function with balancing provided by a regularization parameter, λ. Deterministic algorithms for the optimization, such as Levenberg-Marquardt or Gauss-Newton, require the use of derivative information of the objective function, and find the minimum of the non-linear objective function. They will not, however, necessarily distinguish between global and local minima, (Zeyen and Pous, 1993). Convergence to a local minimum is likely and is particularly dependent on the initial model. As an alternative, optimization based on a controlled random search can be used (Montana, 1994). Algorithms in this class, such as simulated annealing and natural genetic selection, simulate naturally-occurring phenomena and do not require any derivative information for the objective function. Here, we use the genetic algorithm (GA) which employs a random search algorithm based on the mechanisms of natural selection and natural genetics.

*Overview of main scientific contributions.*Bijani et al. (2015) introduced the use of graph theory for the three-dimensional inversion of gravity data. Our approach implements and extends the algorithm. (i) Weighting of the data misfit term is introduced using knowledge of the noise in the measured data. (ii) An effective technique for determining λ based on a regression (data fitting) analysis of the convergence curves for the equidistance stabilizing function with a statistical measurement of the reliability of the data fitting is presented. (iii) The inversion algorithm is available as open source MATLAB code and provides multiple options for picking the parameters of the GA. (iv) An accompanying script for generating a synthetic model is provided. This work, therefore, realizes the original proposal of Bijani et al. (2015) as a tool for the general inversion of three-dimensional gravity data arising due to a single dominant homogeneous subsurface target. The algorithm is open source and available at https://math.la.asu.edu/~rosie/research/gravity.html, along with a full description of the algorithm implementation and example simulations.

The paper is organized as follows. In Section 2.1 we present the forward model for the gravity data, leading immediately to the inversion formulation to be solved using the GA, as described in Section 2.2. The specific GA is presented algorithmically in Algorithm 1 and necessary components of the graph theory are also provided. Section 3 describes how the presented Matlab software can be used to both generate data and perform the inversion. The use of the software is illustrated in Section 4.1, with a discussion of regression analysis to find λ in Section 4.2. Finally, in Section 4.3, results are presented for the application of the method on gravity data from the Mobrun ore body, north east of Noranda, Quebec, Canada.

2. Inversion methodology

In this section we briefly review the gravity inversion based on graph theory. For more details the readers should refer to Bijani et al. (2015).

2.1. The forward model

Suppose a point mass in the subsurface is located at point Q and has coordinates $\mathbf{r}_j = (x_j, y_j, z_j)$, Fig. 1. The resulting vertical component of the gravity field at point P on the surface with coordinates $\mathbf{r}_i = (x_i, y_i, z_i)$ is given by, (Blakely, 1995),

$$g_z(\mathbf{r}_i, \mathbf{r}_j) = -\gamma \frac{m_j(z_i - z_j)}{||\mathbf{r}_i - \mathbf{r}_j||_2^3}. \tag{1}$$

Here γ is the universal gravity constant, m_j is the value of the mass

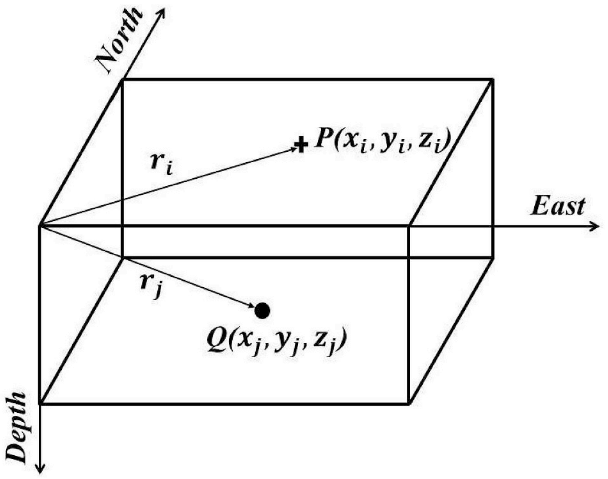

Fig. 1. A single point mass located in the subsurface at point Q which has coordinates $\mathbf{r}_j = (x_j, y_j, z_j)$. Point P is the gravity station located at the surface with coordinates $\mathbf{r}_i = (x_i, y_i, z_i)$.

assigned to point Q, and $\|.\|_2$ indicates the Euclidean norm of a vector. The total vertical gravity component at point P due to M point masses in the subsurface is obtained by superposition over all point masses and is given by

$$(\mathbf{g}_z)_i = \sum_{j=1}^{M} g_z(\mathbf{r}_i, \mathbf{r}_j). \tag{2}$$

Here $(\mathbf{g}_z)_i$ denotes the i^{th} component of the vector $\mathbf{g}_z \in \mathscr{R}^N$ which comprises the responses at all stations $i = 1: N$ on the surface, and describes the forward gravity model. Inversion of the model requires the estimation of the total mass of points and their positions given the measurements of the gravity anomaly at the N gravity stations. The estimated set of point masses indicates a skeleton of the geometry and provides the total mass of the causative subsurface source relative to the background mass of the surrounding area, (Bijani et al., 2015).

2.2. The inverse model

Suppose that the observed gravity data for a homogeneous source are given by the components of the vector $\mathbf{g}_{\text{obs}} \in \mathscr{R}^N$ and that the point masses, randomly spread throughout the domain, have the same mass, $m_j = m_p$ for all j. Then, the total mass is assumed to be $m_t = Mm_p$. Suppose that the Cartesian coordinates of the sources are assigned to vector $\mathbf{p} \in \mathscr{R}^{3M}$ ordered as

$$\mathbf{p} = (x_1, y_1, z_1, \cdots, x_M, y_M, z_M)^T, \tag{3}$$

and that the resulting vector of model parameters of dimension $3M + 1$ is given by

$$\mathbf{q} = (m_t, \mathbf{p}^T)^T. \tag{4}$$

It is desired to find vector $\mathbf{q}$ which generates forward vector $\mathbf{g}_z(\mathbf{q})$ that predicts the observed gravity vector $\mathbf{g}_{\text{obs}}$ at the given noise level. The data fitting constraint is imposed using the data-misfit term in the weighted Euclidean norm

$$\Phi(\mathbf{q}) = \|W_{\mathbf{d}}(\mathbf{g}_{\text{obs}} - \mathbf{g}_z(\mathbf{q}))\|_2^2, \tag{5}$$

with a diagonal data weighting matrix $W_{\mathbf{d}}$, with entries $(W_{\mathbf{d}})_{ii} = \sigma_i^{-1}$ where σ_i^2 is the assumed variance of the error in the i^{th} measurement $(\mathbf{g}_{\text{obs}})_i$ (Li and Oldenburg, 1998). Equivalently it is assumed that the noise in the data is Gaussian and uncorrelated, and $W_{\mathbf{d}}$ is the inverse square root of the diagonal covariance matrix for the noise.

The non-uniqueness of the gravity inversion problem, and the associated sensitivity of the solution to noise in the data, requires that the set of potential solutions $\mathbf{q}$ that minimize $\Phi(\mathbf{q})$ is reduced by the introduction of a stabilization term in the minimization. Bijani et al. (2015) introduced the use of concepts from graph theory for stabilizing the solution of (5). First, suppose that the point masses are considered as vertices of a complete[6] graph with the edges between the vertices connecting all the point masses, Fig. 2a. For edge between vertices i and j a weight d_{ij} is assigned. In this case, d_{ij} is the Euclidean distance between point masses i and j. Thus closer points have a smaller weight. Imposing M point masses, the minimum spanning tree (MST) problem finds the graph that connects all point masses while minimizing the total distance in the graph, namely it forms the least distance spanning tree (LDST) for the graph, Fig. 2b. The number of edges of the LDST for M point masses is $M - 1$. Kruskal's algorithm, (Kruskal, 1956), is a greedy algorithm for finding the subset of edges that form the LDST. We use $\mathbf{d}^{MST}(\mathbf{p}) \in \mathscr{R}^{M-1}$ to denote the vector containing the lengths of all edges of the LDST, and $\bar{d}^{MST}(\mathbf{p})$ to be the mean of the lengths of the edges of the MST. Then, as a further stabilization of the search space, the MST is constrained to have edges of approximately equal length yielding the stabilizing equidistance function

$$\Theta(\mathbf{p}) = \sum_{i=1}^{M-1} [d_i^{MST}(\mathbf{p}) - \bar{d}^{MST}(\mathbf{p})]^2, \tag{6}$$

where $d_i^{MST}(\mathbf{p})$ is the length of edge i for vector $\mathbf{d}^{MST}(\mathbf{p})$, (Bijani et al., 2015). Here $\Theta(\mathbf{p})$ effectively minimizes the variance in the edge lengths against their average and thus biases the solution toward a homogeneous 3D spatial distribution of point sources from a single structure in the subsurface. Consequently, the inversion algorithm is able to reconstruct the skeleton of the subsurface body.

Given the data misfit function Φ and the stabilization term Θ, a balancing parameter, or regularization parameter, λ, is introduced. This trades off the relative importance of the data misfit and stabilization terms in the objective function

$$\Gamma(\mathbf{q}) = \Phi(\mathbf{q}) + \lambda\Theta(\mathbf{p}). \tag{7}$$

An algorithm is required to obtain $\mathbf{q}_{\text{opt}}$ that minimizes Γ for a fixed λ. Further, an approach is required that efficiently selects a λ which generates an acceptable solution given the measured data.

Bijani et al. (2015) suggested a genetic algorithm for the minimization of $\Gamma(\mathbf{q})$, (Goldberg and Holland, 1988; Montana, 1994, e.g.). The method starts from an initial random population, consisting of a number of individuals $\mathbf{q}$, and iteratively improves the estimated solution. At each iteration each individual of the population is given a fitness (i.e., a value of the objective function $\Gamma(\mathbf{q})$). The fittest individuals are selected for reproduction in order to produce offspring that replace the least fit individuals of the current iteration. The population size is thus fixed. A small percentage of this new population is arbitrarily mutated, dependent on a given mutation rate, so different areas of the search space can be explored. This assists with avoiding local minima in the optimization process. The new population is also evaluated, allowing only the fittest individuals to survive, and the process is repeated. Constraints on the model parameters (Cartesian coordinates and total mass) are used in all stages of the GA, allowing the inclusion of prior information on the model.

The standard termination criterium for potential field data inversion is that the algorithm iterates until the weighted data misfit, Φ, satisfies the χ^2 test. This is an estimate of how well the current estimate predicts the data and thus indicates that the obtained solution predicts the data up to the noise level in the data (Boulanger and Chouteau, 2001). We thus terminate the GA when either the solution satisfies the noise level,

[6] For a complete graph all vertices are connected.

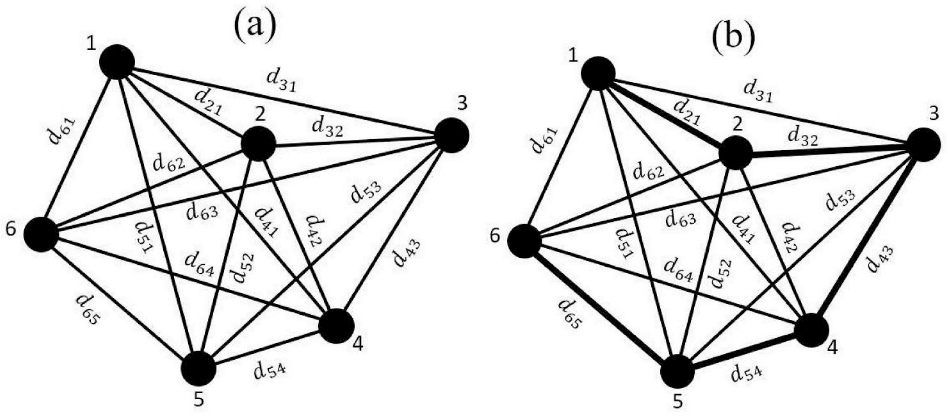

Fig. 2. (a) An example of a complete graph with 6 vertices (point masses numbered from 1 to 6). d_{ij} is the Euclidean distance between point masses i and j; (b) The LDST obtained by Kruskal's algorithm. The elected edges are specified by bold black lines. Then, the vector $\mathbf{d}^{MST}$ contains [d_{21}, d_{32}, d_{43}, d_{54}, d_{65}].

$$\Phi(\mathbf{q}) = \|W_{\mathbf{d}}(\mathbf{g}_{\text{obs}} - \mathbf{g}_z(\mathbf{q}))\|_2^2 \leq N + \sqrt{2N}, \tag{8}$$

or a certain number of generations, $K_{\max}$, is reached. The best individual of all generations is selected as the final estimate, $\mathbf{q}_{\text{opt}}$. The inversion methodology for a fixed λ is summarized in Algorithm 1.

Algorithm 1. IGUG: Minimization of $\Gamma(\mathbf{q})$ for gravity inversion using a genetic algorithm, given measured data $\mathbf{g}_{\text{obs}}$ and estimated noise distribution on the data via $W_{\mathbf{d}}$.

```
Require: Genetic algorithm parameters as detailed in Table 7.
for $\ell = 1$ to noq do
    Generate random population $\mathbf{q}^{(\ell)}$. Impose coordinate and mass constraints:
    $x_{\min} \leq x_j \leq x_{\max}$, $y_{\min} \leq y_j \leq y_{\max}$, $z_{\min} \leq z_j \leq z_{\max}$, $m_{t_{\min}} \leq m_t \leq m_{t_{\max}}$.
end for
$k = 0$. $\Phi(\mathbf{q}_{\text{opt}}) = 10^6$.
while $(k < K_{\max})$ & $(\Phi(\mathbf{q}_{\text{opt}}) > N + \sqrt{2N})$ do
    for $\ell = 1$ to noq do
        Generate a complete graph for $\mathbf{q}^{(\ell)}$. Use Kruskal's algorithm to find the least
        distance spanning tree for $\mathbf{q}^{(\ell)}$. Calculate $\mathbf{d}^{MST}(\mathbf{q}^{(\ell)})$ and $\overline{d}^{MST}(\mathbf{q}^{(\ell)})$. Compute
        $\Gamma(\mathbf{q}^{(\ell)}) = \Phi(\mathbf{q}^{(\ell)}) + \lambda\Theta(\mathbf{p}^{\ell})$.
    end for
    $\mathbf{q}_{\text{opt}} = \arg\min_{\ell} \Gamma(\mathbf{q}^{(l)})$.
    Use GA to generate a new population via genetic selection, mutation and crossover.
    Impose bound constraints at all stages.
end while
Ensure: $\mathbf{q}_{\text{opt}}$ and iteration count $k$.
```

We reiterate that Algorithm 1 is non deterministic due to the use of the genetic algorithm. Running for a fixed data set, and fixed choice of parameters, as detailed in Table 7, does not provide an exactly reproducible result. Furthermore, we note that for iterative regularization algorithms a possibility that may be considered is to minimize with λ also decreasing iteratively. This, however, introduces additional parameters for the algorithm and thus here we follow the approach introduced in Bijani et al. (2015), which obtains a solution for a fixed λ. Moreover, we present an approach to obtain a suitable solution from solutions obtained for a range of λ.

3. Code availability and software package

The software consists of three main scripts.

GMD.m: is used to generate a synthetic model and its gravity data subject to a user-specified survey area and subsurface geometry. It can also be used to create the appropriate real data set for inversion, using the measured data, noise distribution and survey area.

IGUG.m: loads the data file produced for either synthetic or real data and performs the inversion to find $\mathbf{q}_{\text{opt}}$. It can be run for a single λ, or a range of values for λ.

Diagnostic_Results.m: is used to analyze the results and provides an approach for determining λ. It is included at the end of IGUG.m and is also a standalone script for analyzing output from IGUG.m.

Extensive discussion on each script is available in the documentation, including specifics on the input and output parameters. This information also discusses the directory structure and provides examples of the usage of the package. We review the important components of these main scripts below.

3.1. GMD.m

MD.m is an easy to use MATLAB code for producing the vertical component of the gravity field, the data vector $\mathbf{g}_{\text{obs}}$, for a user defined synthetic model at a specified noise level. The model is generated using an ensemble of one or more prisms. For example, a vertical dike may need just one prism, but a more complex but connected geometry is represented by a set of prisms. The parameters of the simulation, including the survey volume, subsurface geometry, noise variance for $W_{\mathbf{d}}$ and all parameters required for the inversion are saved for import to the inversion module IGUG.m. GMD.m can be edited by the user for more

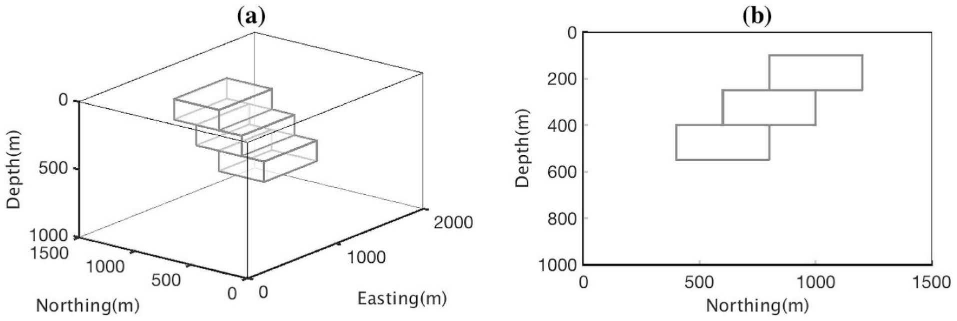

Fig. 3. Model of a dipping dike with density contrast of 1 g/cm^3. (a) A perspective view of the model; (b) The cross-sectional view of the model.

general usage when generating synthetic data sets, and in particular to modify the model for the noise.

GMD.m can also be used to read a real data file with the measured data set that includes the data vector $\mathbf{g}_{\text{obs}}$, an estimate for $W_{\mathbf{d}}$ and the coordinates for the locations of the stations. In this case the user is asked to provide the additional parameters that are required for the inversion, including the survey volume and the parameters required for the inversion, but does not assume any knowledge of the subsurface geometry.

For both synthetic and real data sets GMD.m provides a plot of the survey volume and the gravity anomaly, and in the case of synthetic data the subsurface geometry is inset within the survey volume. This allows the user to check that the information has been correctly provided. The outline for GMD.m when used for synthetic data sets is provided in Algorithm 2. A simple modification is coded for the case with real data.

Algorithm 2. GMD: Generating a synthetic model: In all cases default values may bechosen.

```
Require: Initial exact gravity data is empty. $\mathbf{g}_{\text{exact}} = []$
Generate the survey domain: Provide coordinates of the origin, extension of the volume
  in East, North and depth dimensions.
Data for generating the anomaly: Give distances between stations in East and North
  directions and number of prisms, noc, used for the subsurface structure. Pick a noise
  level index: $j$.
for $k = 1$ to noc do
    Define the substructure Give the three-dimensional coordinates and the density of
      prism $k$.
    Generate the gravity anomaly for prism $k$: $\mathbf{g}_{\text{exact}}^{(k)}$
    Accumulate exact gravity: $\mathbf{g}_{\text{exact}} = \mathbf{g}_{\text{exact}} + \mathbf{g}_{\text{exact}}^{(k)}$
end for
Generate noisy gravity anomaly and provide noise distribution: $\mathbf{g}_{\text{obs}}$ and $W_{\mathbf{d}}$.
Check data input: Plot true and noisy data and the subsurface geometry.
Ensure: Save parameters $\mathbf{g}_{\text{obs}}$, $W_{\mathbf{d}}$, discretization choices, and survey area descriptions to
  DataNj.mat.
```

3.2. IGUG.m

IGUG.m implements the inversion methodology based on Algorithm 1. It requires a synthetic data set such as produced using GMD.m or can be used for real data with the same format, potentially also generated using GMD.m as noted in Section 3.1. Parameters for the GA must also be given, as indicated in Table 7. The constraint conditions on the horizontal coordinates can be defined by analyzing the amplitude of the observed data. The constraints for the total mass and the depth coordinates can be determined from prior information. Our experience indicates that it is not necessary to determine tight constraints. Thus, when no prior information is available wide constraints still provide acceptable results. It is possible to use all parameters of the GA set to default values, but the user is interrogated as to whether values should be altered.

3.3. Diagnostic_Results.m

Diagnostic_Results.m can be used to assist in interpretation of the results of the genetic algorithm and to select the parameter λ. The user has the option to plot obtained results for visual inspection without any further analysis, if all dialogue boxes are answered with "No". In this case plots are given of $(k, \Gamma(k))$, $(k, \Phi(k))$ and $(k, \log(\Theta(k))$ for each choice of λ and the resulting point mass distribution will be provided within the survey volume. A table of results that summarizes the final values of k, Γ, $\Phi/(N + \sqrt{2N})$ and Θ for the given λ is displayed in the command window.

As we will see from the data, when λ is too small, instability in the convergence of Θ with increasing k is indicative of a solution that is under-regularized, or that the solution is not progressing and Θ is at the noise level for the computation. This can be assessed applying a standard regression analysis. Thus, for the diagnostics we also present the option to do a regression analysis for Γ, Φ and $\log(\Theta)$ as a function of k, yielding a R^2 value which is indicative of the goodness of fit. The user may also select the range for k to use for the regression analysis, which is otherwise set as $[\min(75, \text{floor}(K_{\max}/2)), K_{\max}]$. In comparing results for the same data and same choice for M, but different choices for λ, regression analysis gives a quantitative measure that indicates in which case the decay of $\log(\Theta)$ is most stable; not wildly oscillating. Then, the linear regression lines are also illustrated in the plots and the R^2 values given in the table of results. We will show how these results can be used to efficiently estimate an appropriate choice for λ at limited cost. Finally there is the option to save all figures in.jpg format, and to export the table of results to a spread sheet.

Table 1
The dimensions of the prisms used to form the model in Fig. 3.

Prism	East (m)	North (m)	Depth
Upper	700 to 1300	800 to 1200	100 to 250
Middle	700 to 1300	600 to 1000	250 to 400
Lower	700 to 1300	400 to 800	400 to 550

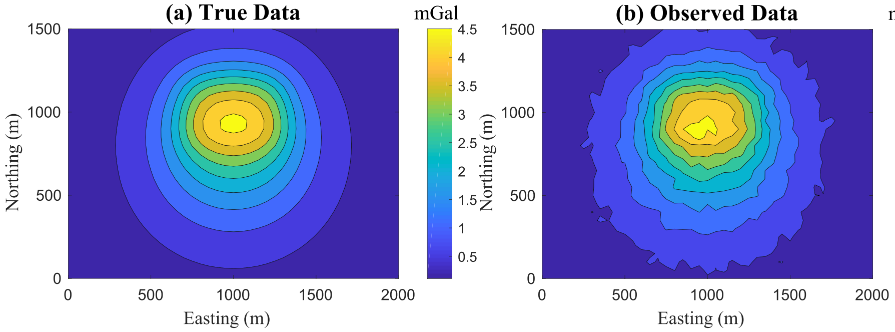

Fig. 4. The gravity anomaly produced by the model shown in Fig. 3, without noise in Fig. 4a and contaminated by noise with $\sigma_i = (0.02(\mathbf{g}_{\text{exact}})_i + 0.001\|\mathbf{g}_{\text{exact}}\|_2)$ in Fig. 4b.

Table 2
Parameters used as input of Algorithm 1 to perform inversion for data of Fig. 4. Coordinates are given in meters, *m*, and mass in kilograms, *kg*.

noq	$x_{\min}$	$x_{\max}$	$y_{\min}$	$y_{\max}$	$z_{\min}$	$z_{\max}$	$m_{t\min}$	$m_{t\max}$
100	400	1600	100	1400	20	1000	70*e*9	150*e*9

Table 3
The results of the inversion for the given selections of λ, *M* and $K_{\max}$. In all cases $\Phi(\mathbf{q}_{\text{opt}}) > N + \sqrt{2N} \approx 1321$ at the final iteration.

Figure	λ	*M*	$\Phi(\mathbf{q}_{\text{opt}})$	$m_t(kg)$	$K_{\max}$	Time (seconds)	R^2
5	100	20	63209	89.7*e*9	200	117.6	.9883
6	.1	20	2254	119.7*e*9	200	121.1	.8942
7	.00001	20	1483	115.6*e*9	200	117.2	.3377
8	.1	20	1609	115.4*e*9	1000	589.9	.5949
9	.1	40	3372	130.2*e*9	200	176.4	.8874

4. Results

We present results using the software package for the inversion of both simulated and real data sets, Sections 4.1, 4.2 and 4.3, respectively. All reports on timing are presented for an implementation using MATLAB Version 9.4.0.813654 (R2018a) running under the Mac OS X Version: 10.13.6 Operating System. These results can be replicated using the simulated and real data sets DataN4.mat and AllRealData.mat that are provided with the codes, but it should be noted that all results depend on randomization in the GA and thus obtained results will be equivalent but not exact replications. We reiterate that the problem is ill-posed and there is no unique solution even for a fixed choice of λ. In our experiments we mainly present results with the assumption of 20 point masses in the domain, consistent with the recommendation in Bijani et al. (2015). For comparison, however, we show some results for $M = 40$ to verify the properties of the algorithm. Additional results showing simulations with $M = 10$, 20 and 40 are available at the accompanying web page https://math.la.asu.edu/~rosie/research/gravity/htmlruns/SimulatedData.

4.1. Synthetic example

We consider the example of a dipping dike model, Fig. 3. GMD.m was used to generate the model for a dike with three prisms, noc = 3. The dimensions of the prisms are given in Table 1. The density contrast of the dike is 1 g/cm^3 and its total mass is 108×10^9 kg. Gravity data of the model, $\mathbf{g}_{\text{exact}}$, were generated on the surface for a grid of $41 \times 31 = 1271$ points with grid spacing 50 m. As standard for the generation of synthetic data for evaluating inversion algorithms, Gaussian noise with standard deviation $(0.02(\mathbf{g}_{\text{exact}})_i + 0.001\|\mathbf{g}_{\text{exact}}\|_2)$ is added to each datum yielding the noisy data set, $\mathbf{g}_{\text{obs}}$, illustrated in Fig. 4, (Li and Oldenburg, 1998). The selected parameters for performing the inversion are given in Table 2 and a summary of the results is provided in Table 3.

We contrast the results for choices of λ that lead to under- and over-regularization, and show the impact of increasing the number of iterations and number of point masses. In each case we illustrate in figures (a)-(d) resp., a perspective view of the point masses; the cross-sectional view of the point masses; the equidistance function for the best solution at each iteration; and the data predicted by the reconstructed model. When λ is relatively large, $\lambda = 100$ in Fig. 5a-d, the product $\lambda\Theta$ initially dominates in Γ. Thus the algorithm forces Θ to become small and iterates toward a solution for which but the data misfit Φ is not significantly reduced; a local minimum of Θ yields a dispersed set of point masses that does not give a skeleton of the body. Comparing the results using moderate $\lambda = .1$ and very small $\lambda = .00001$, Fig. 6a-d and Fig. 7a-d, respectively, we can see that the solution for smaller λ is more dispersed in depth after 200 iterations, and that there is significant oscillation in Θ with *k*. This occurs because the small value of λ places less emphasis on minimizing Θ with increasing *k* and instead forces Φ to decrease more quickly. Notice that $\log(\Theta) \approx O(6)$, $O(11)$, after 200 iterations, respectively. Thus at 200 iterations Θ is much larger for small $\lambda = .00001$, Θ≈ 50000 as compared to 500 for $\lambda = .1$.

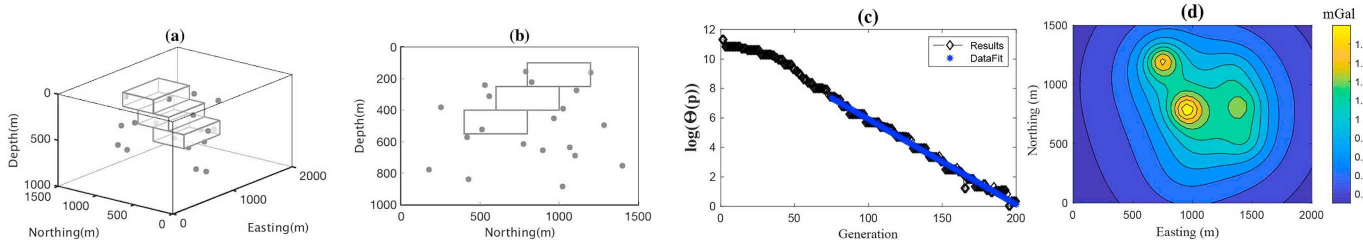

Fig. 5. Inversion results with $\lambda = 1 \times 10^2$, $K_{\max} = 200$ and $M = 20$.

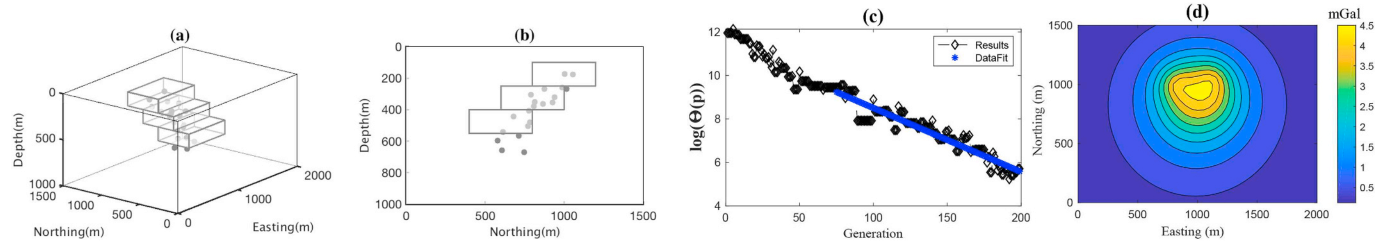

Fig. 6. Inversion results with $\lambda = .1$, $K_{\max} = 200$ and $M = 20$.

Increasing the number of iterations but still using moderate $\lambda = .1$, Fig. 8a-d, we can see that the algorithm continues to decrease Φ while the rate of decrease in Θ slows, between 200 and 1000 iterations Θ decreases only from approximately 500 to 50, but stably, and the distribution of point masses is not modified significantly. Thus taking additional steps is relatively costly, increasing the computational cost by a factor 5 going from 200 to 1000 steps with little gain. Finally, it remains to assess whether the solution is significantly impacted by increasing the number of point masses, Fig. 9a-d. Because Θ depends on the number of point masses, the decrease in Θ with k, and hence of Φ with k, is slower when M is larger, reaching only $\Theta \approx 8000$ after 200 steps. Thus after just 200 iterations the solution has not converged to an acceptable solution, the points are dispersed but overall Θ is decaying in a stable manner. Increasing the number of allowable iterations to 1000 for $M = 40$ in this case will give a stable and satisfactory solution.

Contrasting the predicted anomalies, Figs. 5d, 6d and 7d with Fig. 4a, it is clear that the over-regularized result (large λ) does not yield a good approximation. Moreover, considering the quantitative results in Table 3, for large λ the total mass is under-estimated. Thus,

Table 4
The results of the inversion of the model for the given selections of λ, $M = 20$ and $K_{\max} = 200$. The total time for the inversions reported in the table is 1452.2 s, or approximately 24 min.

λ_i	k	mass	$\Theta(k)$	$\Phi(k)$	$\Phi(k)/(N+\sqrt{2N})$	R^2
100	200	$112.6e+9$	17.486	54315	41.1	0.88
10	200	$83.8e+9$	9.86	75172	56.9	0.93
1	200	$141.4e+9$	70.517	11427	8.65	0.91
0.5	200	$120.0e+9$	109.03	4746.8	3.59	0.96
0.25	200	$127.5e+9$	202.24	3646.8	2.76	0.95
0.1	200	$119.7e+9$	381.8	2129.8	1.61	0.95
0.05	200	$118.0e+9$	373.48	1898.4	1.44	0.86
0.025	200	$122.5e+9$	1262	2492.2	1.89	0.94
0.01	200	$116.9e+9$	3858.4	1608.6	1.22	0.88
0.001	200	$114.2e+9$	14654	1484.0	1.12	0.86
0.0001	200	$118.0e+9$	51524	1512.3	1.14	0.01
0.00001	200	$117.9e+9$	300060	1543.2	1.17	0.38

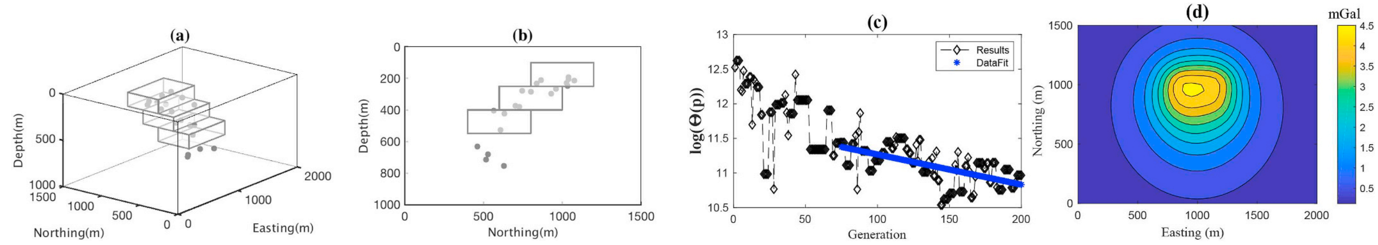

Fig. 7. Inversion results with $\lambda = 1 \times 10^{-5}$, $K_{\max} = 200$ and $M = 20$.

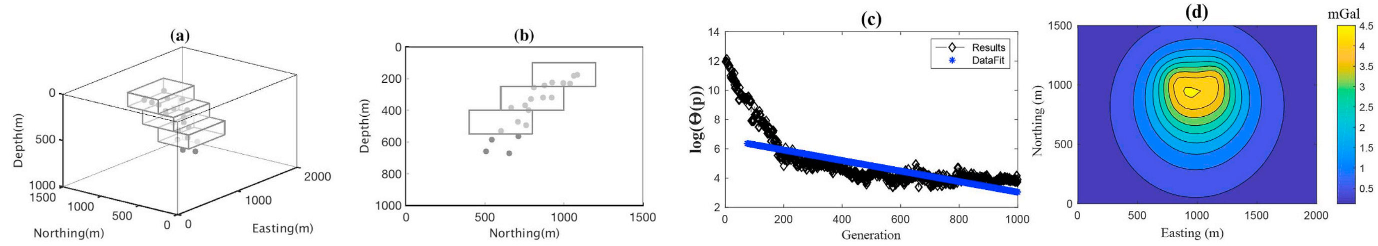

Fig. 8. Inversion results with $\lambda = .1$, $K_{\max} = 1000$ and $M = 20$.

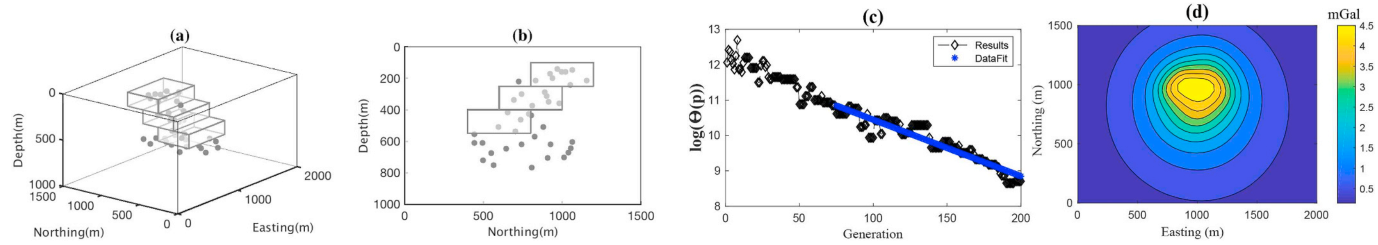

Fig. 9. Inversion results with $\lambda = .1$, $K_{\max} = 200$ and $M = 40$.

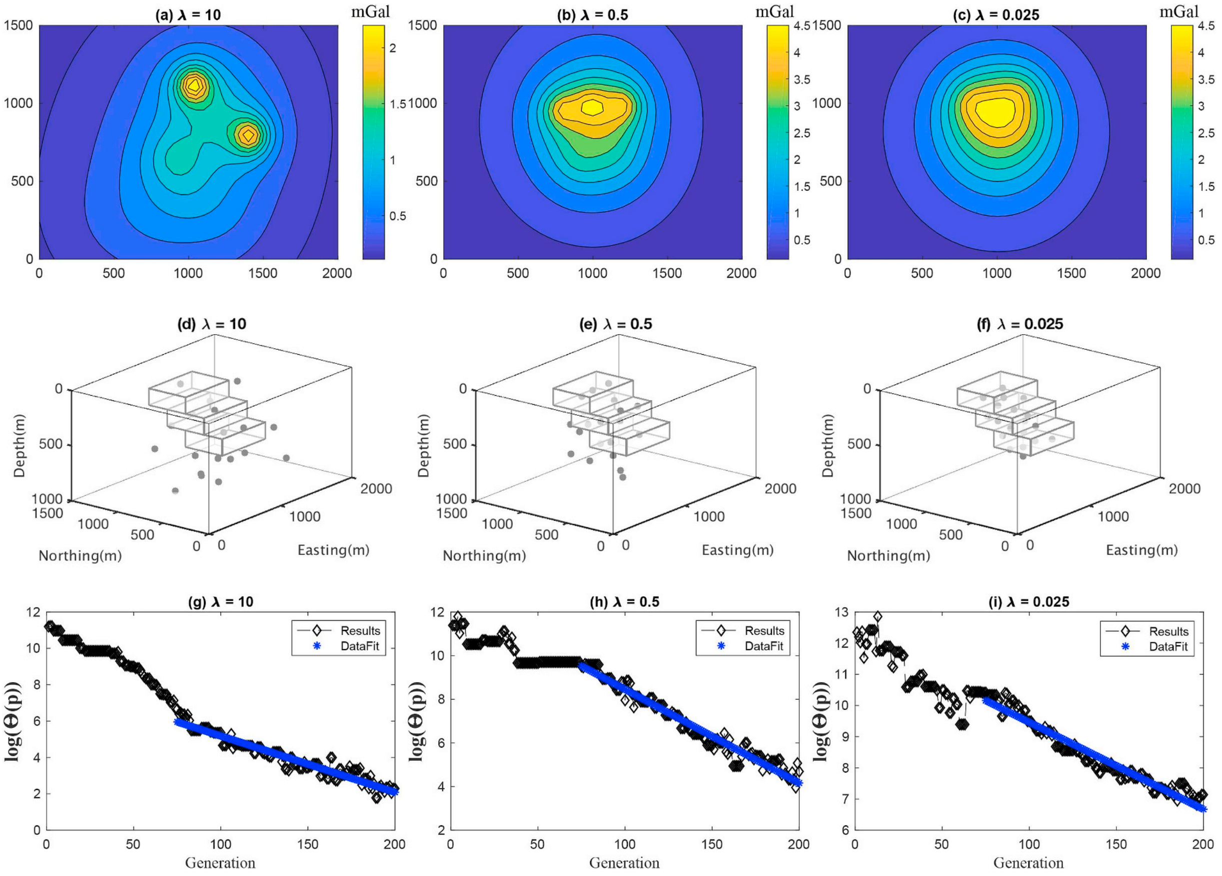

Fig. 10. The point masses distributions, the predicted anomalies and Θ with the indicated regression line (data fit) for the solutions chosen according to the data in Table 4.

although in most cases the mass is over-estimated, we cannot conclude that the mass estimate will always be an over-estimate. From these results, we conclude that while the final value of Φ is closer to the desired estimate $N + \sqrt{2N} \approx 1321$ for $\lambda = .00001$, the lack of stability in the estimate of Θ with k, as indicated by the low R^2 value suggests that the convergence is not stable, and that this result would be less reliable than the choice with $\lambda = .1$. It should be noted that the computational cost is effectively independent of λ, all timings are on the order of 120 s, for the determination of the solution, with fixed $M = 20$ and $K_{\max} = 200$.

In summary, the characteristics of the solutions shown are consistent with minimizing Γ that is dependent on parameters M and λ. Increasing M slows the iteration due to the graph based algorithm, and changing λ impacts the balance of the terms in Γ, leading to potential over-and under-regularization. This is no different than we would expect from other methods of regularization with increasing resolution, M, and varying stabilization parameter λ. From the presented results, we conclude that when (i) there is a small data misfit Φ and when (ii) $\Theta(\mathbf{p})$ exhibits stable convergence, the solution is neither over-nor under-regularized, and the reconstructed point mass distribution for the given λ provides a good approximation of the skeleton of homogeneous source. Thus, in general, the optimum parameter can be estimated without running the code for a large number of values of λ, as is required for example with the L-curve approach suggested by Bijani et al. (2015).

4.2. Applying diagnostics to determine λ

We now discuss an assessment tool implemented in Diagnostic_Results.m that can be used to automatically analyze the results based on a regression analysis. This provides a computationally efficient method to identify a λ that provides a solution that is neither under- nor over-regularized, without performing the extensive computation required to generate an $L-$ curve. First the computations demonstrate that while Φ decays linearly with k both Γ and Θ decay proportionally to $A\exp(-k)$, and thus to assist with assessing quality of the solution regression analysis is applied for $\log(\Theta)$ as function of k.[7] For purposes of space, we only show the plots for the decay of $\log(\Theta)$ with k, plots for regression analysis for Φ and Γ are available for these examples on the software web page, and it is easy to generate a data fit for the exponential of these functions also.

Table 4 gives the results for model simulations obtained for all the parameters as given in Tables 1 and 2 for the simulation data illustrated in Fig. 4b, an inversion with 20 mass points, maximum iteration $K_{\max} = 200$ and the noted range of λ_i. From the results in Table 4 it is evident that the convergence behavior of Θ is stable for large λ; R^2 is close to 1 but Φ is large relative to the noise level and the mass estimation is not stable, the mass may be underestimated. Further, for large λ the solution terminates with small Θ. The R^2 value eventually decreases, on average, as λ decreases before increasing again at the choice of Φ which is closest to the noise estimate. These results suggest that an acceptable solution will be obtained for λ ranging from about 0.1 to 0.025. We illustrate the resulting point masses distributions for $\lambda = 10$, 0.5, and 0.025 in Fig. 10, demonstrating that the analysis is relevant. There are also links to simulated data sets giving several analyses of

[7] Note that we use the MATLAB notation $\log(x)$ to denote the natural logarithm of x, and consistent with the exponential decay rate. $\log_{10}(x) = \log(x)/\log(10) \approx .4\log(x)$.

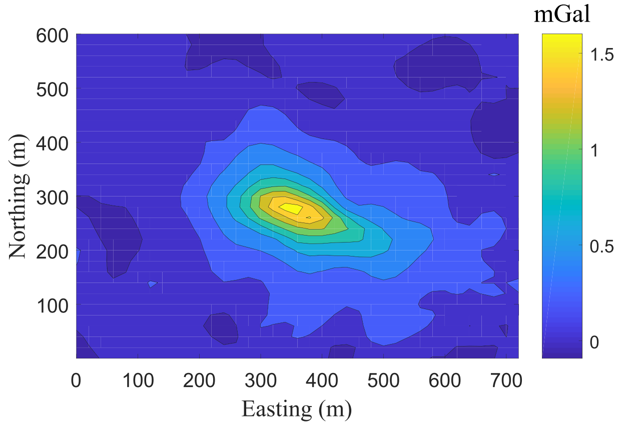

Fig. 11. Residual anomaly of Mobrun ore body, Noranda, Quebec, Canada.

Table 5
Parameters used in Algorithm 1 to perform inversion on data of Fig. 11. Coordinates are given in meters, *m*, and mass in kilograms, *kg*.

M	$K_{\max}$	noq	$x_{\min}$	$x_{\max}$	$y_{\min}$	$y_{\max}$	$z_{\min}$	$z_{\max}$	$m_{t_{\min}}$	$m_{t_{\max}}$
20	200	100	150	650	50	500	10	300	$2.2e9$	$3.2e9$

data for multiple choices of λ, M and noise levels in the accompanying webpage. We also note that we do not present this analysis to suggest that the user would wish to evaluate the solution for a large set of λ, here 12 values, rather the intent is to demonstrate that the impact of λ on the solution is significant and that the R^2 value is a useful estimator even if the solution is obtained for a small set of λ choices.

4.3. Real data

To illustrate the relevance of the approach for a practical case we applied the software to reconstruct the well-known Mobrun ore body, northeast of Noranda, Quebec, Canada, Fig. 11. The anomaly pattern is associated with a massive body of base metal sulphide (mainly pyrite) which has displaced volcanic rocks of middle Precambrian age (Grant and West, 1965). We carefully digitized the data from Fig. 10.1 in Grant and West (1965), and re-gridded onto a regular grid of $37 \times 31 = 1147$ data in east and north directions respectively, with grid spacing 20 m. We approximate the error distribution with $\sigma_i = (0.03(\mathbf{g}_{\mathrm{obs}})_i + 0.004\,\|\mathbf{g}_{\mathrm{obs}}\|_2)$. Grant and West (1965) interpreted the body to be about 305 m in length, slightly more than 30 m in maximum width and having a maximum depth of 183 m. Furthermore, they estimated the total mass of the body to be $2.56e9$ kg. The parameters of Algorithm 1 for the inversion are detailed in Table 5.

We performed the inversion with several fixed values of λ and here show the diagnostic results obtained using the selection $\lambda = [10, .25, .001]$ in Table 6. The resulting point masses distributions and anomalies support the selection of $\lambda = .25$ for the acceptable result, Fig. 12.

Table 6
The results of the inversion for real data. The total time for the inversion for all values of λ is 509 s.

λ_i	k	mass	$\Theta(k)$	$\Phi(k)$	$\Phi(k)/(N+\sqrt{2N})$	R^2
10	200	$2.51e+9$	2.4959	9563.2	8.00	0.70
0.25	200	$3.18e+9$	44.376	1910.6	1.60	0.93
0.001	200	$3.13e+9$	21657	1485.4	1.24	0.42

5. Conclusions

We have presented MATLAB software for 3D inversion of gravity data using an equidistance stabilization term based on a graph theory argument that was developed by Bijani et al. (2015). The subsurface homogeneous body is approximated by a set of point masses that provide a skeleton of a subsurface structure. The point masses are associated with a complete graph and Kruskal's algorithm is used to find the minimum spanning tree of the graph. The equidistance stabilization term restricts the spatial distribution of the point masses and suggests a homogeneous spatial distribution of connected point masses in the subsurface. The global objective function is minimized using a genetic algorithm using crossover, mutation and random population initialization, with a priori constraints on the parameters imposed at all stages of the population evolution. A module for generating a synthetic geometry and gravity data set is also provided. The software is user-friendly and can be modified to use for practically acquired data sets and simulations of synthetic data. It is open source software and available at Vatankhah et al. (2018).

The software was illustrated for a physically realistic test problem with Gaussian noise added to the gravity measurements. The objective function includes a regularization parameter which balances the relative importance of the data misfit and the equidistance stabilization during the optimization. It was demonstrated that a suitable choice of regularization parameter is one for which (i) the predicted data are close to the observed data relative to the noise level and (ii) the equidistance function decays almost monotonically with increasing numbers of iterations. Thus it is sufficient to carry out the optimization for relatively few choices of λ, particularly when similar data sets have been previously analyzed and an acceptable range for the regularization parameter has been found. A new statistical approach based on regression analysis has been illustrated and assists with identification of λ when no prior data sets have been analyzed.

The methodology was illustrated for gravity data from the Mobrun ore body. The maximum extensions of the body in the east and north directions were found to be approximately 350 m and 200 m, respectively, and are in good agreement with results from previous investigations and from drill hole information.

Acknowledgements

R.A. Renaut acknowledges the support of NSF grant DMS 1418377 “Novel Regularization for Joint Inversion of Nonlinear Problems”. We sincerely appreciate the very insightful comments of an unknown referee. The paper was improved by the comments.

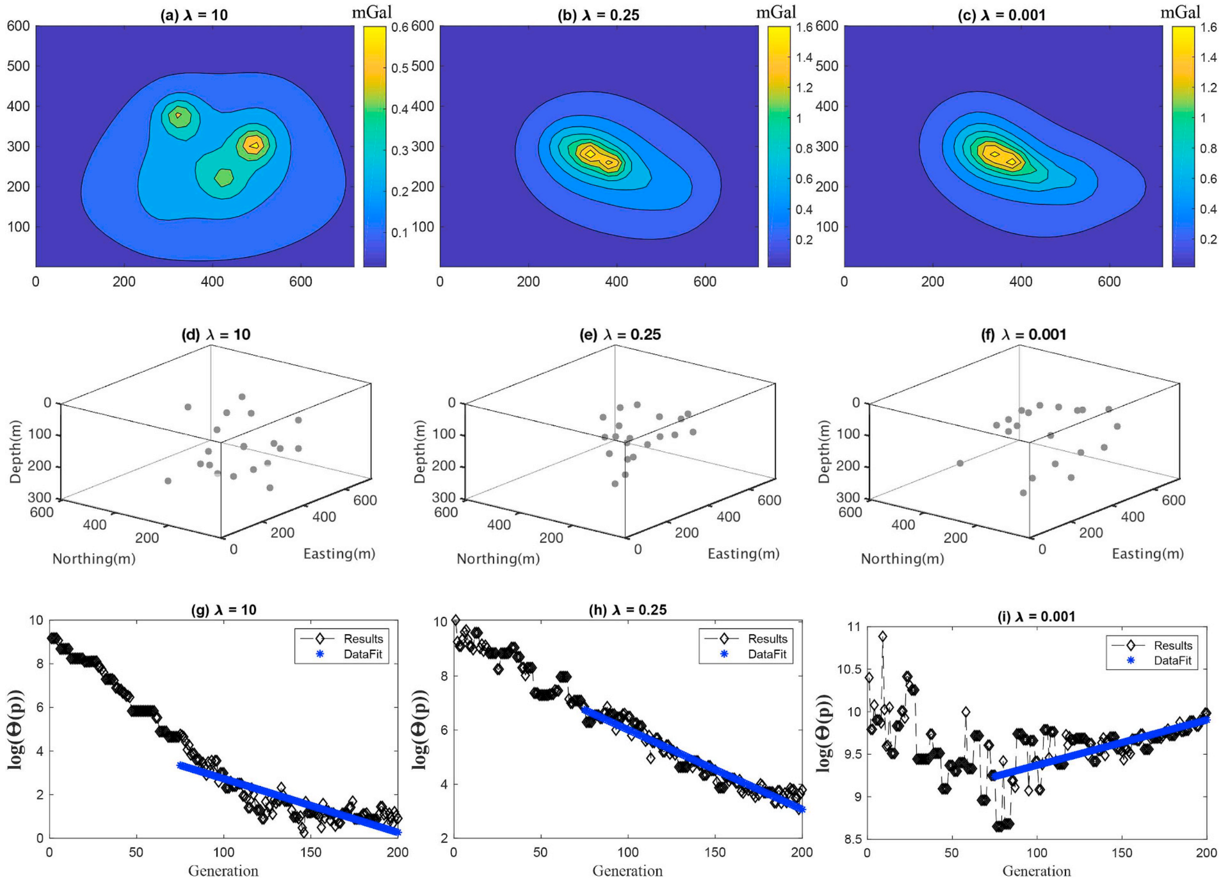

Fig. 12. The point masses distributions, predicted anomalies and Θ with the indicated regression line (data fit) for the solutions chosen according to the data in Table 5 for the real data illustrated in Fig. 11.

Appendix A. Supplementary data

Supplementary data to this article can be found online at https://doi.org/10.1016/j.cageo.2019.03.008.

Appendix A. Genetic Algorithm Parameters

Table 7
Input Parameters used for the Genetic Algorithm.

Population Size	noq
Max Generations	$K_{\max}$
Cross Over Percentage	CP
Extra Range Factor for Crossover	Errf
Mutant Percentage	MP
Mutation Rate	μ
Selection Pressure	β
Number of Point Masses	M
Minimum total mass	$m_{t_{\min}}$
Minimum in East Direction	$x_{\max}$
Minimum in North Direction	$y_{\max}$
Minimum in Depth Direction	$_s$
Maximum total mass	$m_{t_{\max}}$
Maximum in East Direction	$x_{\max}$
Maximum in North Direction	$y_{\max}$
Maximum in Depth Direction	$z_{\max}$

References

Bijani, R., Ponte-Neto, C.F., Carlos, D.U., Silva Dias, F.J.S., 2015. Three-dimensional gravity inversion using graph theory to delineate the skeleton of homogeneous sources. Geophysics 80, G53–G66.

Blakely, R. j., 1995. Potential Theory in Gravity and Magnetic Application. Cambridge University Press, Cambridge.

Bott, M.H.P., 1960. The use of rapid digital computing methods for direct gravity interpretation of sedimentary basins. Geophys. J. R. Astron. Soc. 3, 6367.

Boulanger, O., Chouteau, M., 2001. Constraint in 3D gravity inversion. Geophys. Prospect. 49, 265–280.

Chakravarthi, V., Sundararajan, N., 2007. 3D gravity inversion of basement relief- A depth-dependent density approach. Geophysics 72 (2), I23–I32.

Goldberg, D.E., Holland, J.H., 1988. Genetic algorithms and machine learning. Mach. Learn. 3, 95–99.

Grant, F.S., West, G.F., 1965. Interpretation Theory in Applied Geophysics. McGraw-Hill.

Kruskal Jr., J.B., 1956. On the shortest spanning subtree of a graph and the traveling salesmann problem. Proc. Am. Math. Soc. 7, 48–50.

LaFehr, T.R., Nabighian, M.,N., 2012. Fundamentals of Gravity Exploration. Society of Exploration Geophysicistshttps://doi.org/10.1190/1.9781560803058.

Last, B.J., Kubik, K., 1983. Compact gravity inversion. Geophysics 48, 713–721.

Li, Y., Oldenburg, D.W., 1998. 3-D inversion of gravity data. Geophysics 63, 109–119.

Liu, S., Hu, X., Xi, Y., Liu, T., Xu, S., 2015. 2D sequential inversion of total magnitude and total magnetic anomaly data affected by remanent magnetization. Geophysics 80 (3), K1–K12.

Martins, C.M., Lima, W.A., Barbosa, V.C.F., Silva, J.B.C., 2011. Total variation regularization for depth-to-basement estimate: Part 1 Mathematical details and applications. Geophysics 76 (1), I1–I12.

Montana, D.J., 1994. Strongly typed genetic programming. Evol. Comput. 3, 199–230.

Portniaguine, O., Zhdanov, M.S., 1999. Focusing geophysical inversion images. Geophysics 64, 874–887.

Vatankhah, S., Ardestani, V.E., Niri, S.S., Renaut, R.A., Kabirzadeh, H., 2018. Description of IGUG: A MATLAB Program for 3-D Inversion of Gravity Data Using Graph Theory. https://math.la.asu.edu/~rosie/research/gravity.html.

Vatankhah, S., Ardestani, V.E., Renaut, R.A., 2015. Application of the X^2 principle and unbiased predictive risk estimator for determining the regularization parameter in 3-D focusing gravity inversion. Geophys. J. Int. 200, 265–277.

Vatankhah, S., Renaut, R.A., Ardestani, V.E., 2017. 3-D Projected L1 inversion of gravity data using truncated unbiased predictive risk estimator for regularization parameter estimation. Geophys. J. Int. 210 (3), 1872–1887.

Zeyen, H., Pous, J., 1993. 3-D joint inversion of magnetic and gravimetric data with a priori information. Geophys. J. Int. 112, 244–256.